SIMP-Method Topology Optimization of Ferrite Structures in Inductive Power Transfer Systems

Yao Pei, Lionel Pichon, Yann Le Bihan, and Mohamed Bensetti

***Abstract*—This article demonstrates the interest of topology optimization in designing the ferrite plate used in an inductive power transfer system for electric vehicles. The solid isotropic material with the penalization (SIMP) method is used to optimize the ferrite plate, and it modifies the topology of the ferrite shape iteratively. This SIMP method can lead to novel structures compared with usual existing shapes. In this article, it is found that a part of the ferrite from the center and the edges of the predefined ferrite plate can be removed to save the ferrite volume while achieving a minimal reduction of transmission efficiency. Moreover, the results from topology optimization are influenced by the aluminum shielding plate near the ferrite plate. Hence, the ferrite on the receiver side has to be larger than the one on the transmitter side. These results give some design guidelines on arranging the ferrite placement for the system, and the approach could be generalized for shielding sheets/walls.**

***Index Terms*—Inductive power transfer (IPT) system, shielding optimization, topology optimization (TO).**

I. Introduction

THE electrification of transportation means has taken importance in recent years, especially in the automotive domain, where the problems of global warming are driving manufacturers to find cleaner solutions that are more respectful of the environment. However, promoting and adopting plug-in electric vehicles (EVs) raises many questions. First, the cost of lithium batteries is high. Second, the batteries are heavy. Third, the charging time for the battery is so long that it requires an expensive infrastructure for charging stations [1], [2], [3]. The use of inductive power transfer (IPT) charging systems is a promising solution. In such a system, the energy is transferred wirelessly between two coils (constituting the coupler) through the magnetic field. However, this inevitably causes electromagnetic field (EMF) leakage around the system [1], [2], [3], [4], [5].

Manuscript received 24 April 2023; revised 20 July 2023; accepted 24 August 2023. Date of publication 15 September 2023; date of current version 13 December 2023. *(Corresponding author: Yao Pei.)*

Yao Pei and Mohamed Bensetti are with the CentraleSupélec and Laboratoire de Génie Electrique et Electronique de Paris, 91192 Gif-sur-Yvette, France (e-mail: yao.pei@centralesupelec.fr; mohamed.bensetti@centralesupelec.fr).

Lionel Pichon is with the Centre National de la Recherche Scientifique and Laboratoire de Génie Electrique et Electronique de Paris, 91192 Gif-sur-Yvette, France (e-mail: lionel.pichon@centralesupelec.fr).

Yann Le Bihan is with the University Paris-Saclay and Laboratoire de Génie Electrique et Electronique de Paris, 91192 Gif-sur-Yvette, France (e-mail: yann.lebihan@geeps.centralesupelec.fr).

Color versions of one or more figures in this article are available at https://doi.org/10.1109/TEMC.2023.3311632.

Digital Object Identifier 10.1109/TEMC.2023.3311632

To mitigate the effects of EMF leakage, shielding is usually added in IPT systems, thus improving the system performance and leading to better efficiency [4], [5], [6]. Different types of shielding have been reported in the literature. In [7], [8], and [9], the extra coil turns wounded in the reverse direction to create a magnetic field in a reverse direction to the original magnetic field created by the coupler to minimize the EMF leakage. Moon et al. [10] incorporated additional reactive components (e.g., capacitors) and coil turns close to the transmitter coils for the shielding. Lee et al. [11] designed a soft-magnetic-metal-based shield structure to reduce magnetic flux leakage. Recently, a hybrid shielding structure has been proposed by surrounding a reactive *LC* coil with a ring-based aluminum plate, which weakens EMF leakage around the system [12].

Among the types of shielding mentioned above, ferrite materials are commonly used in IPT systems due to their high permeability and low electrical conductivity [1], [2], [3], [4], [5], [6]. Ferrite structures contribute to the shielding effectiveness of the system. The permeability and the losses of the ferrite material determine the magnetic field strength and hence the transmission efficiency of the system. Then, optimizing the ferrite topology can lead to significant improvements in the efficiency of the IPT system.

Recent literature proposes some parameter optimization methods used for the ferrite design of IPT systems [13], [14], [15], [16], [17], and for optimizing structural parts in antenna systems [18], [19], [20], [21]. Although combining 3-D finite element methods (FEM) with optimization algorithms provides a systematic, iterative process, it leads to heavy computations. To reduce the overall cost, a metamodel, such as sparse polynomial chaos expansions (PCE), can be used in the iterative procedure to deal with multiobjective optimization [22], [23]. With such an approach, the computational burden can be strongly reduced. However, in these previous parametric optimization works, the general shape of the ferrite structures remains the same and follows some predefined shapes (rectangular, for example). This does not allow innovative ferrite structures. To face such limitations, topology optimization (TO) appears as a powerful computational technique that can be used to optimize the design of ferrite materials in IPT systems [24], [25], [26], [27]. It involves iteratively modifying the topology of the ferrite material while ensuring that certain performance criteria are met. The performance criteria may include the magnetic field strength, the energy transfer efficiency, or the losses in the ferrite material [28]. The main TO methods are the solid isotropic material with the penalization (SIMP) method [29], the ON–OFF method [30],

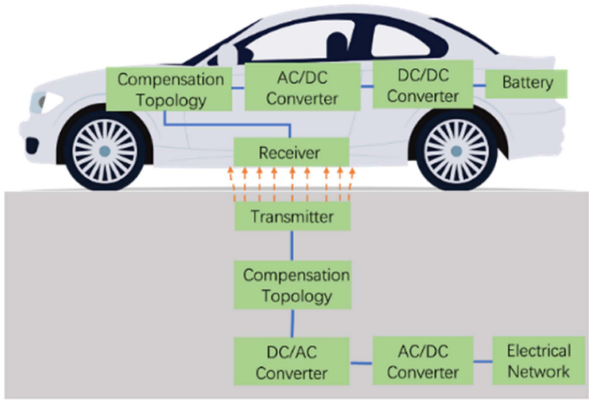

Fig. 1. IPT system.

and others [31]. The main advantage of TO is that it can lead to novel structures, but it is limited by the predefined investigation area.

In [24] and [25], the coil and magnetic-core shapes are optimized using the ON–OFF method with the aid of a genetic algorithm and 3-D FEM so that the coupling coefficient of the IPT system is maximized. Otomo and Igarashi [26] proposed a TO method for the IPT system using the geometry projection method to generate the bar-shaped magnetic cores. In [27], TO is applied with the SIMP method to optimize the ferrite structure for circular couplers. Although these papers optimize the ferrite installed on circular/double-D couplers, they do not consider how the ferrite structure varies under different ferrite volume constraints (and then the cost of the system), and they do not give any guidelines to arrange the ferrite placement.

The interest of this work is to find a design guideline for the ferrite distribution that maximizes the transmission efficiency, while constraining the volume of the ferrite plate, obtaining a light and cost-effective IPT system. TO with SIMP method is the most commonly used one due to its easy and intuitive implementation [29], [31], and it is adopted to generate different ferrite structures in two situations (without a shielding aluminum plate above the receiver [22], and with a shielding aluminum plate above the receiver [23]). The system has been previously studied in our lab by coupling optimization algorithms with the sparse PCE technique. The results obtained from TO could give some design guidelines for the ferrite arrangement during the design process of the IPT system.

The rest of this article is organized as follows. Section II provides a general description of IPT systems for EVs and gives some equations about transmission efficiency. Section III presents an overview of TO and how it works with ferrite structures. Some results are presented and discussed. Finally, Section IV concludes this article.

II. IPT System

Fig. 1 shows the block diagram of an IPT system, which is the most attractive for EVs. The system comprises a transmitter, a receiver, converters, and resonant compensation topologies. It is based on ampere's and Faraday's laws in a time-harmonic regime

TABLE I
Parameters and IPT Operating Status

Parameter	Value [Unit]
Transferring power	2.5 [kW]
Operating frequency f_0	85 [kHz]
Transmitting coil current	42 [A RMS]
Air gap between coils	150 [mm]

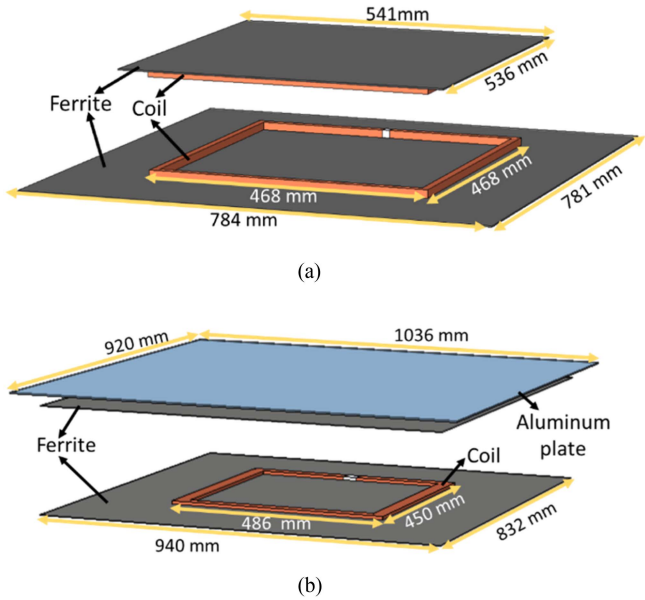

Fig. 2. Arrangement of the transmitter and the receiver. (a) Without an aluminum plate [22]. (b) With an aluminum plate [23].

[4]. First, the electrical network provides a dc-link voltage through the ac/dc converter to feed the transmitter. Then, the magnetic field produced by the transmitter is coupled with the receiver to induce voltages and currents. The induced power is rectified to charge the EV battery. Compensation topologies (such as series–series, parallel–parallel, series–parallel, and parallel–series) are connected to the transmitter and the receiver to create the resonant case and reduce additional losses [3], [4], [5]. The operating parameters of the system considered in this article are listed in Table I [32], [33].

Normally, the transmitter and the receiver consist of copper coils and ferrite plates. However, relying on the ferrite plates for the shielding is not only expensive but also ineffective and heavy for the receiver installed on the EVs [3], [4], [23]. Therefore, to solve this problem, several solutions are proposed: one solution [22] is to design the ferrite on the receiver side appropriately in Fig. 2(a), and the other solution [23] is to add an aluminum plate above the receiver to mitigate the magnetic field generated by the transmitter, as shown in Fig. 2(b). It can also help to decrease the power losses in the vehicle chassis. Although the sizes of the coils are different in the figure, the total coil area is the same, and the turns of the coils are both equal to six. The ferrite thickness is 2 mm, and they are made of 3C95 material from

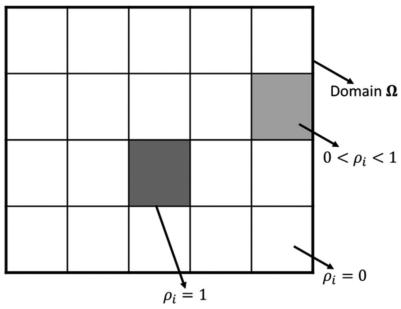

Fig. 3. Domain Ω discretization with SIMP method [27], [31].

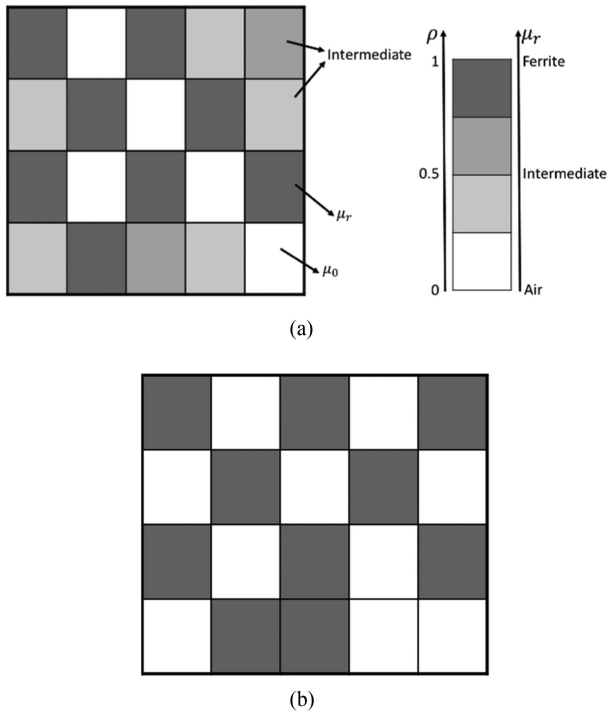

Fig. 4. Ferrite placement with TO on SIMP method. (a) TO process on SIMP method. (b) TO result.

Ferroxcube [34], and its value of the saturation induction (B_s) is around 500 mT.

For analyzing the IPT system transmission efficiency, circuit models are often used, and the compensation topologies are designed to minimize the reactive component of the electrical circuit. Following [3], [4], and [5], the series–series compensation topology is considered because the resonance condition in this compensation remains constant, independently of the variations of the mutual inductance and the load. Therefore, the relationship between the maximum transmission efficiency $\eta_{\max}$ and the mutual inductance M between coils can be described in the following equation when the transmitter coil and the receiver coil are identical [35]:

$$\eta_{\max} = 1 - \frac{R_1}{\pi f_0 M} \tag{1}$$

where R_1 is the resistance of the transmitter as same as that of the receiver.

III. Topology Optimization

Although the dimensions of the ferrite can be easily selected by parametric optimization, however, it is limited to how to arrange the ferrite part in the specified size properly. So, to solve this problem, TO is used to find a ferrite distribution that maximizes the mutual inductance M, while constraining the volume of the ferrite plate, obtaining a light design for the IPT system. The basic idea of TO is to modify the topology of the ferrite shape iteratively. Changing the value of the local relative permeability allows the introduction of holes in the ferrite plate. Although there are several TO methods in the literature, the SIMP method is adopted to arrange the ferrite distribution in this section.

A. Introduction to SIMP-Based TO

The SIMP method discretizes a studied domain Ω into numerous elements, for which artificial density values are introduced as design variables ρ_i, as illustrated in Fig. 3. ρ_i is the material density in the ith element. The artificial density value of ρ_i lying between 0 and 1, represents a proportion of solid material or void. It is desired to have either solid material ($\rho_i = 1$), or void ($\rho_i = 0$) as the final material in the element instead of having intermediates (unless intermediates are materials that are available for the users) [27], [31]. The material properties between the solid and void are interpolated with a smooth continuous function, which depends on the material density ρ_i.

Then, as it is desired here to optimize the topology of the ferromagnetic materials, the adequate choice is to consider only permeability as the material property. So, the function of the ferrite's relative permeability μ_r is achieved in the following equation [27], [29], [31], [36], [37]:

$$\mu_{r_i} = \mu_{r0} + (\mu_r - \mu_{r0})\,\rho_i^n \tag{2}$$

where μ_r is the relative permeability of ferrite, equal to 3000 and μ_{r0} is the relative permeability of air, equal to 1, and $0 \le \rho_i \le 1$. The penalization coefficient n, (usually set between 2 and 5) is used to change the interpolation behavior with $n \ge 1$, and it works on the design variable ρ_i. The gradient-based optimization solver is used to find a good solution, and each variable is allowed to take the relative permeability of either ferrite (μ_r) or air (μ_{r0}) so as to maximize the objective function [27], [31], [36], [37]. Fig. 4(a) shows the initial domain to be optimized, where each discretization represents a variable of the problem, and the color legend for the materials, with the corresponding ρ and μ_r. The TO result should be composed of ferrite and air, as shown in Fig. 4(b).

In this section, the objective function of the ferrite placement optimization, under the defined ferrite volume constraint, is to minimize the ratio α

$$\alpha = \frac{M_{\text{initial ferrite domain}}}{M_{\mu_{r_i}\ \text{optimized ferrite domain}}} \tag{3}$$

where $M_{\text{initial ferrite domain}}$ represents the mutual inductance with the initial ferrite design domain and

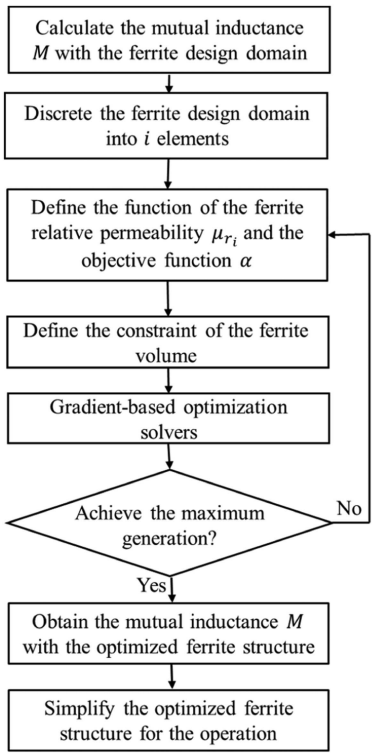

Fig. 5. Flowchart of TO in the ferrite placement.

$M_{\mu_{r_i}\text{ optimized ferrite domain}}$ represents the ith mutual inductance with the ith ferrite structure. The optimization process is based on the assumption that the ferrite is not in the saturation state [27], [29].

The process for the TO on the ferrite placement is presented in Fig. 5.

The constraint of ferrite volume can be defined manually, but the optimization of the ferrite placement aims at minimizing the reduction in the value of the mutual inductance M compared with M with the initial ferrite domain. The TO result allows some ferrite parts to be removed. The penalization coefficient n is set to 4, which is suggested by some authors in order to produce no intermediate values for μ_r [27], [31].

B. TO Applied to the Ferrite Plate

Here, the ferrite structure is discussed in two situations: without an aluminum plate above the receiver [see Fig. 2(a)] and with an aluminum plate above the receiver [see Fig. 2(b)]. The TO process works with the optimization module [38] from COMSOL 5.6 on an Intel Xeon W-2125 processor.

1) Without an Aluminum Plate: In order to further save ferrite volume and keep nearly the same mutual inductance, TO with SIMP method is used to find an efficient arrangement of ferrite. The initial dimension of the ferrite plate from Fig. 2(a) and the ferrite structure resulting from the TO optimization under different volume constraints are shown separately in Fig. 6.

The relationship between the ferrite volume and the mutual inductance is shown in Fig. 7.

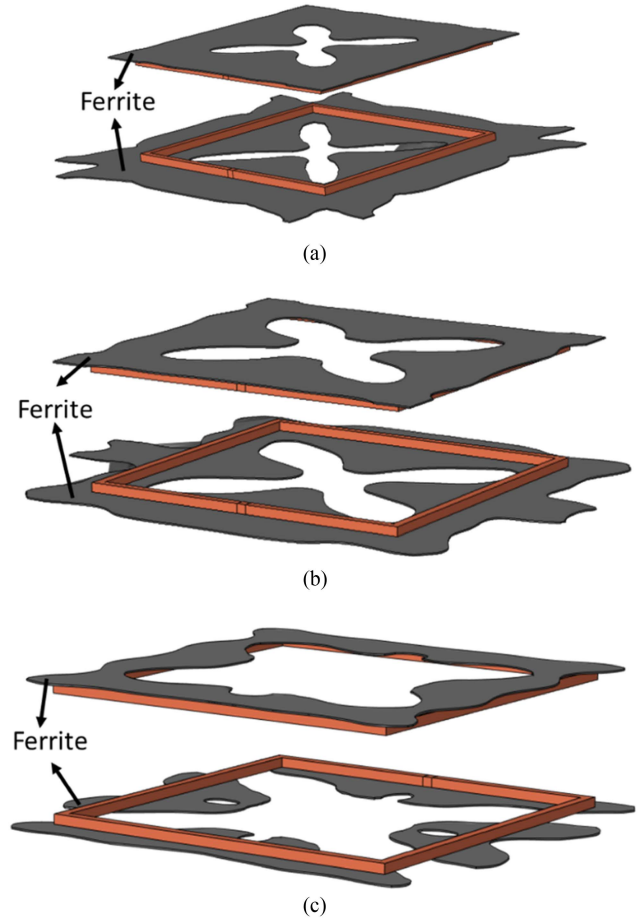

Fig. 6. Ferrite placement without an aluminum plate. (a) Structure from TO under 70% of the ferrite volume. (b) Structure from TO under 50% of the ferrite volume. (c) Structure from TO under 30% of the ferrite volume.

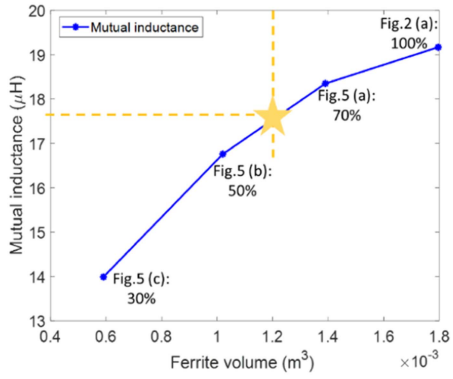

Fig. 7. Relationship between the ferrite volume and the mutual inductance.

Then, it can be observed that during the TO process, removing a part of the ferrite from the center and the edges of the ferrite plates is recommended, no matter the constraint of the ferrite volume ratio. Arranging the ferrite plates with this tip can facilitate a 40% reduction of the ferrite volume, as labeled by the yellow star in Fig. 7. Besides, it also has an approximate 10% reduction in the mutual inductance.

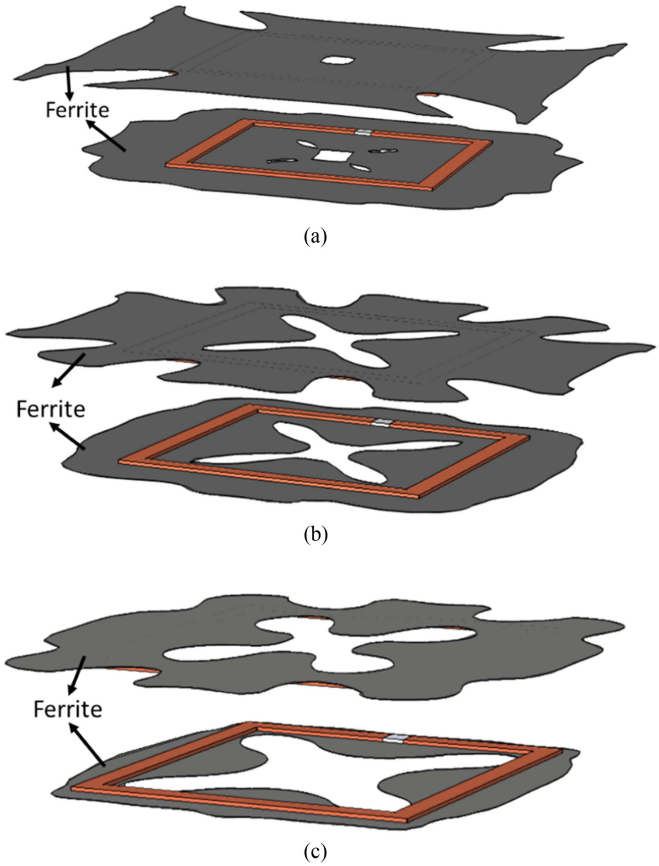

Fig. 8. Ferrite placement with an aluminum plate. (a) Structure from TO under 70% of ferrite volume (the aluminum plate is hidden). (b) Structure from TO under 50% of ferrite volume (the aluminum plate is hidden). (c) Structure from TO under 30% of ferrite volume (the aluminum plate is hidden).

2) With an Aluminum Plate: Even in the case of an aluminum plate above the receiver, the previous optimization procedure can also provide an appropriate arrangement of ferrite for saving ferrite volume and keeping nearly the same mutual inductance. The initial dimension of the ferrite plate from Fig. 2(b) and the ferrite structure under different volume constraints are presented separately in Fig. 8.

It shows that during the TO process, a part of the ferrite from the center and the edges of the ferrite plates should be removed no matter the constraint of the ferrite volume ratio. However, due to the effect of the aluminum plate, the ferrite on the receiver side has to be larger than that on the transmitter side.

Then, the relationship between the ferrite volume and the mutual inductance is summarized in Fig. 9.

Compared with Fig. 2(b), the ferrite structure Fig. 7(a) saves almost 30% of ferrite, but the mutual inductance decreases by around 10%.

C. Discussion

TO, with the SIMP method, provides a quite original ferrite placement. A part of the ferrite from the center and the edges of the ferrite design domain can be removed to decrease the volume and keep a minimal reduction of the mutual inductance

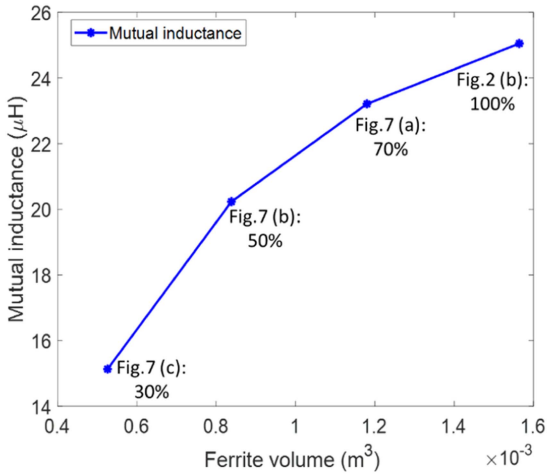

Fig. 9. Relationship between ferrite volume and mutual inductance.

(compared with the one calculated with the initial ferrite design domain) when the transmitter and the receiver are aligned. However, the results from TO are influenced by the aluminum plate near the ferrite design domain. With the existence of the aluminum plate, the ferrite on the receiver side has to be larger than that on the transmitter side.

The structures from the optimization procedure have to be further simplified because the TO results cannot be easily manufactured in reality. Then, the following features that can be deduced from how ferrite should be placed in a manufactural form [24], [25], [26], [27], [31].

1) The optimized ferrite structures are similar but not entirely symmetrical plates. This is due to the optimization randomness. In practice, the placement of the ferrite should be symmetrical, as the coils are rectangular and identical. Therefore, the ferrite should be simplified as symmetrical.
2) The appearance of curves is inevitable in TO. Therefore, curves will be approximated by straight lines or stair-case lines for simplification and operability. Ferrites are commercially available as small tiles and bars. The curved boundaries of the shapes obtained as theoretical results have to be approximated according to the size of the tile/bar.

The present work shows an interest in the distribution of ferrite for IPT systems. Some researchers propose using ferrite bars instead of the ferrite plate for the IPT systems [3], [4], [5], [39]. In [40], the radial ferrite core is distributed on the receiver side, as shown in Fig. 10(a). The center and the edges of the ferrite corner are removed, and they are made from tiles of ferrite material, which satisfies the manufacturing rules. In our GeePs laboratory, for example, the ferrite bars are distributed as illustrated in Fig. 10(b). The ferrite's center is empty, and two sides of the plate are arranged by ferrite bars. Fig. 10(a) and (b) have an arrangement of ferrite bars similar to the TO results. Our optimization procedure gives a possible theoretical explanation of the ferrite shapes used in practice.

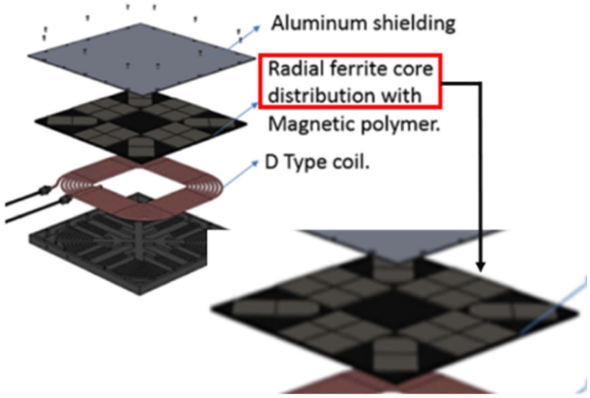

(a)

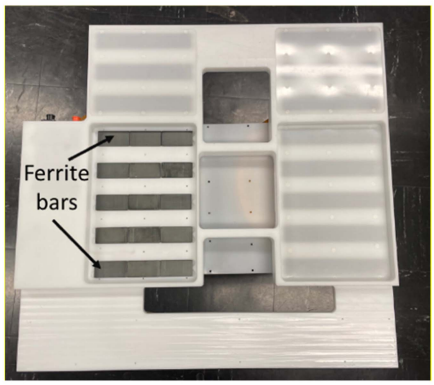

(b)

Fig. 10. Ferrite placement for IPT systems. (a) Radial ferrite core [40]. (b) Ferrite bars.

IV. Conclusion

This article shows that TO of ferrite materials in IPT systems is a promising approach for improving the efficiency of these systems. By optimizing the design of the ferrite material, it is possible to keep nearly the same power transmission efficiency and reduce the overall size, weight, and cost of the system compared with those obtained with traditional approaches. By discussing the ferrite structures of the IPT system without an aluminum plate and with an aluminum plate, decreasing 30% of the ferrite volume leads to only a 10% reduction of the mutual inductance. It is also found that a part of the ferrite from the center and the edges of the predefined ferrite plate can be removed to save the ferrite volume while achieving a minimal reduction of the mutual inductance value. Moreover, the results from TO are influenced by the aluminum plate near the ferrite design domain, so the ferrite on the receiver side has to be bigger than the one on the transmitter side. However, if the TO results are planned to be used in reality, they need to be further simplified for the manufacture. Current ferrite structures can be explained as resulting from TO. Finally, the approach described in this work can be applied to the design of any shielding plate. Furthermore, for high-power IPT systems, additional constraints, such as magnetic flux density distribution, can be added to the optimization process.

References

[1] M. Yilmaz and P. T. Krein, "Review of battery charger topologies, charging power levels, and infrastructure for plug-in electric and hybrid vehicles," *IEEE Trans. Power Electron.*, vol. 28, no. 5, pp. 2151–2169, May 2013.

[2] C. T. Rim and C. Mi, "Wireless power transfer for electric vehicles and mobile devices | IEEE eBooks | IEEE Xplore," 2022. Accessed: Sep. 25, 2022. [Online]. Available: https://ieeexplore-ieee-org.ezproxy.universite-paris-saclay.fr/book/7953908

[3] T. M. Fisher, K. B. Farley, Y. Gao, H. Bai, and Z. T. Tse, "Electric vehicle wireless charging technology: A state-of-the-art review of magnetic coupling systems," *Wirel. Power Transfer*, vol. 1, no. 2, pp. 87–96, 2014.

[4] "Wireless power transfer for electric vehicles: Foundations and design approach," 2022. Accessed: May 12, 2022. [Online]. Available: https://link.springer.com/book/10.1007/978-3-030-26706-3

[5] D. Patil, M. K. McDonough, J. M. Miller, B. Fahimi, and P. T. Balsara, "Wireless power transfer for vehicular applications: Overview and challenges," *IEEE Trans. Transp. Electrific.*, vol. 4, no. 1, pp. 3–37, Mar. 2018.

[6] E. Asa, M. Mohammad, O. C. Onar, J. Pries, V. Galigekere, and G.-J. Su, "Review of safety and exposure limits of electromagnetic fields (EMF) in wireless electric vehicle charging (WEVC) applications," in *Proc. IEEE Transp. Electrific. Conf. Expo*, 2020, pp. 17–24.

[7] T. Campi, S. Cruciani, F. Maradei, and M. Feliziani, "Active coil system for magnetic field reduction in an automotive wireless power transfer system," in *Proc. IEEE Int. Symp. Electromagn. Compat., Signal Power Integrity*, 2019, pp. 189–192.

[8] S. Y. Choi, B. W. Gu, S. W. Lee, W. Y. Lee, J. Huh, and C. T. Rim, "Generalized active EMF cancel methods for wireless electric vehicles," *IEEE Trans. Power Electron.*, vol. 29, no. 11, pp. 5770–5783, Nov. 2014.

[9] T. Campi, S. Cruciani, F. Maradei, and M. Feliziani, "Magnetic field mitigation by multicoil active shielding in electric vehicles equipped with wireless power charging system," *IEEE Trans. Electromagn. Compat.*, vol. 62, no. 4, pp. 1398–1405, Aug. 2020.

[10] H. Moon, S. Kim, H. H. Park, and S. Ahn, "Design of a resonant reactive shield with double coils and a phase shifter for wireless charging of electric vehicles," *IEEE Trans. Magn.*, vol. 51, no. 3, Mar. 2015, Art. no. 8700104.

[11] I.-G. Lee, N. Kim, I.-K. Cho, and I.-P. Hong, "Design of a patterned soft magnetic structure to reduce magnetic flux leakage of magnetic induction wireless power transfer systems," *IEEE Trans. Electromagn. Compat.*, vol. 59, no. 6, pp. 1856–1863, Dec. 2017, doi: 10.1109/TEMC.2017.2690967.

[12] Y. Li, K. Xie, Y. Ying, and Z. Li, "An improved hybrid shielding with LC coil for wireless power transfer system," *IEEE Trans. Electromagn. Compat.*, vol. 64, no. 3, pp. 720–731, Jun. 2022, doi: 10.1109/TEMC.2021.3137527.

[13] M. Budhia, G. A. Covic, and J. T. Boys, "Design and optimization of circular magnetic structures for lumped inductive power transfer systems," *IEEE Trans. Power Electron.*, vol. 26, no. 11, pp. 3096–3108, Nov. 2011, doi: 10.1109/TPEL.2011.2143730.

[14] R. Bosshard, J. W. Kolar, J. Mühlethaler, I. Stevanović, B. Wunsch, and F. Canales, "Modeling and η - α -Pareto optimization of inductive power transfer coils for electric vehicles," *IEEE J. Emerg. Sel. Topics Power Electron.*, vol. 3, no. 1, pp. 50–64, Mar. 2015, doi: 10.1109/JESTPE.2014.2311302.

[15] A. Hariri, A. Elsayed, and O. A. Mohammed, "An integrated characterization model and multiobjective optimization for the design of an EV charger's circular wireless power transfer pads," *IEEE Trans. Magn.*, vol. 53, no. 6, Jun. 2017, Art. no. 8001004, doi: 10.1109/TMAG.2017.2661722.

[16] T. Yilmaz, N. Hasan, R. Zane, and Z. Pantic, "Multi-objective optimization of circular magnetic couplers for wireless power transfer applications," *IEEE Trans. Magn.*, vol. 53, no. 8, Aug. 2017, Art. no. 8700312, doi: 10.1109/TMAG.2017.2692218.

[17] A. A. S. Mohamed, S. An, and O. Mohammed, "Coil design optimization of power pad in IPT system for electric vehicle applications," *IEEE Trans. Magn.*, vol. 54, no. 4, Apr. 2018, Art. no. 9300405, doi: 10.1109/TMAG.2017.2784381.

[18] M. Alibakhshikenari et al., "Improved adaptive impedance matching for RF front-end systems of wireless transceivers," *Sci. Rep.*, vol. 10, no. 1, Aug. 2020, Art. no. 14065, doi: 10.1038/s41598-020-71056-0.

[19] M. Alibakhshikenari et al., "Dual-polarized highly folded bowtie antenna with slotted self-grounded structure for sub-6 GHz 5G applications," *IEEE Trans. Antennas Propag.*, vol. 70, no. 4, pp. 3028–3033, Apr. 2022, doi: 10.1109/TAP.2021.3118784.

[20] W. A. Awan et al., "Design and realization of a frequency reconfigurable antenna with wide, dual, and single-band operations for compact sized wireless applications," *Electronics*, vol. 10, no. 11, Jan. 2021, Art. no. 1321, doi: 10.3390/electronics10111321.
[21] M. Alibakhshikenari, B. S. Virdee, C. H. See, R. A. Abd-Alhameed, F. Falcone, and E. Limiti, "Super-wide impedance bandwidth planar antenna for microwave and millimeter-wave applications," *Sensors*, vol. 19, no. 10, Jan. 2019, Art. no. 2306, doi: 10.3390/s19102306.
[22] Y. Pei, L. Pichon, M. Bensetti, and Y. L. Bihan, "Multiobjective optimization based on polynomial chaos expansions in the design of inductive power transfer systems," *COMPEL-Int. J. Comput. Math. Elect. Electron. Eng.*, vol. 41, no. 6, pp. 2045–2059, Jan. 2022.
[23] Y. Pei, L. Pichon, Y. L. Bihan, M. Bensetti, and P. Dessante, "Fast shielding optimization of an inductive power transfer system for electric vehicles," *IEEE Access*, vol. 10, pp. 91227–91234, 2022, doi: 10.1109/ACCESS.2022.3198953.
[24] Y. Otomo and H. Igarashi, "A 3-D topology optimization of magnetic cores for wireless power transfer device," *IEEE Trans. Magn.*, vol. 55, no. 6, Jun. 2019, Art. no. 8103005, doi: 10.1109/TMAG.2019.2900744.
[25] Y. Gong, Y. Otomo, and H. Igarashi, "Multi-objective topology optimization of magnetic couplers for wireless power transfer," *Int. J. Appl. Electromagn. Mechanics*, vol. 64, no. 1–4, pp. 325–333, Jan. 2020, doi: 10.3233/JAE-209337.
[26] Y. Otomo and H. Igarashi, "Topology optimization of magnetic cores for WPT using the geometry projection method," *COMPEL-Int. J. Comput. Math. Elect. Electron. Eng.*, vol. 41, no. 3, pp. 889–899, Jan. 2021, doi: 10.1108/COMPEL-02-2021-0064.
[27] M. Hu, U. K. Madawala, and C. Baguley, "The optimal placement of ferrite in inductive power transfer coupling pads," in *Proc. IEEE 12th Energy Convers. Congr. Expo. - Asia*, 2021, pp. 469–474. doi: 10.1109/ECCE-Asia49820.2021.9479004.
[28] H. Zhao et al., "Comprehensive investigation on the influence of magnetic materials on the weight and performance of onboard WPT systems," *IEEE Trans. Ind. Appl.*, vol. 58, no. 5, pp. 6842–6851, Sep./Oct. 2022, doi: 10.1109/TIA.2022.3188611.
[29] M. P. Bendsøe and O. Sigmund, "Material interpolation schemes in topology optimization," *Arch. Appl. Mechanics*, vol. 69, pp. 635–654, 1999, doi: 10.1007/s004190050248.
[30] T. Sato, K. Watanabe, and H. Igarashi, "Multimaterial topology optimization of electric machines based on normalized Gaussian network," *IEEE Trans. Magn.*, vol. 51, no. 3, Mar. 2015, Art. no. 7202604.
[31] B. S. B. Mohamodhosen, "Topology optimisation of electromagnetic devices," Theses, Ecole Centrale de Lille, Accessed: Jul. 29, 2022. [Online]. Available: https://tel.archives-ouvertes.fr/tel-01818091
[32] K. Kadem, "Modeling and optimization of a magnetic coupler for dynamic induction charging of electric vehicles," Ph.D. dissertation, Universite Paris-Saclay, Paris, France, 2020. [Online]. Available: https://hal.archives-ouvertes.fr/tel-03253967
[33] K. Kadem, M. Bensetti, Y. L. Bihan, E. Labouré, and M. Debbou, "Optimal coupler topology for dynamic wireless power transfer for electric vehicle," *Energies*, vol. 14, no. 13, Jan. 2021, Art. no. 3983, doi: 10.3390/en14133983.
[34] "Materials-Ferroxcube," 2023. Accessed: Jun. 29, 2023. [Online]. Available: https://www.ferroxcube.com/en-global/ak_material/index/power_conversion
[35] Y. Pei, Y. L. Bihan, M. Bensetti, and L. Pichon, "Comparison of coupling coils for static inductive power-transfer systems taking into account sources of uncertainty," *Sustainability*, vol. 13, no. 11, Jan. 2021, Art. no. 6324, doi: 10.3390/su13116324.
[36] "Performing topology optimization with the density method," COMSOL. Accessed: Sep. 4, 2022. [Online]. Available: https://www.comsol.com/blogs/performing-topology-optimization-with-the-density-method/
[37] M. P. Bendsøe, "Optimal shape design as a material distribution problem," *Struct. Optim.*, vol. 1, pp. 193–202, 1989.
[38] "Optimize your multiphysics models with the optimization module," COMSOL, 2023, Accessed: Jul. 05, 2023. [Online]. Available: https://www.comsol.com/optimization-module
[39] A. A. S. Mohamed, A. A. Shaier, H. Metwally, and S. I. Selem, "A comprehensive overview of inductive pad in electric vehicles stationary charging," *Appl. Energy*, vol. 262, Mar. 2020, Art. no. 114584, doi: 10.1016/j.apenergy.2020.114584.
[40] R. Austin, "PREMO launches high-efficiency secondary coils for wireless charging," Charged EVs, 2019, Accessed: Oct. 28, 2019. [Online]. Available: https://chargedevs.com/newswire/premo-launches-high-efficiency-secondary-coils-for-wireless-charging/

Yao Pei was born in Zhejiang, China, in 1994. She received the Diploma master's degree in electrical energy from Universite de Nantes, Nantes, France, in 2019, and the Ph.D. degree in electrical engineering from Universite Paris-Saclay, Paris, France, in 2022.

She is currently working as a Postdoc with the Group of Electrical Engineering-Paris, Paris, France. She has authored or coauthored several papers in the international journals. Her current research interests include wireless power transfer system, electromagnetic compatibility, optimization, machine learning, and uncertainty analysis.

Lionel Pichon received the Diploma engineering degree in electrical and electronic engineering from the Ecole Supérieure d'Ingénieurs en Electronique et Electrotechnique, Paris, France, in 1984, and the Ph.D. degree in electrical engineering from the Laboratoire de Génie Electrique de Paris, Paris, France, in 1989.

He was with the Centre National de la Recherche Scientifique (CNRS), Paris, France, in 1989. He is currently the Directeur de Recherche (Senior Research Scientist) with the Group of electrical engineering-Paris (GeePs), Paris, France. He has authored or coauthored more than 130 journal articles in peer-reviewed journals. His research interests include computational electromagnetics for wave propagation, wireless power transfer, and electromagnetic compatibility.

Dr. Pichon is working as a Reviewer for several scientific international journals. He is an Associated Editor of the *European Physical Journal-Applied Physics*.

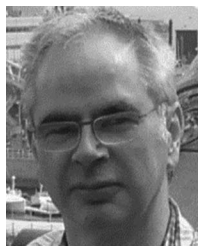

Yann Le Bihan received the engineering degree in electrical engineering and the Ph.D. degree in electronics from the ENS de Cachan, Paris, France, in 1996 and 2000, respectively, and the enabling degree to supervise the Ph.D. studies (HDR) from the Universit é Paris-Sud, Paris, France, in 2007.

From 2001 to 2011, he was an Assistant Professor with IUT de Cachan, Cachan, France, and Universit é Paris-Sud. Since 2011, he has been a Professor with IUT de Cachan. In 2000, he joined the Laboratoire de Génie Electrique de Paris, which became the Group of Electrical Engineering of Paris, Paris, France in 2015. His research interest includes characterization and nondestructive testing by electromagnetic methods: modeling, sensor design, and inverse problems.

Mohamed Bensetti received the master's degree (DEA) in electrical engineering in 2001 and the Ph.D. degree in electrical engineering in 2004 from the University of Paris-Sud, Paris, France, respectively.

From 2005 to 2007, he worked as Researcher with Ecole Supérieure d'Electricité (SUPELEC) – Gif sur Yvette, France. In 2007, he joined Ecole Supérieure d'Ingénieur en Génie Electrique (ESIGELEC), Rouen, France, where he was a Lecturer and Researcher with the Research Institute for Electronic Embedded Systems (IRSEEM). In January 2013, he joined the energy department of SUPELEC. He received the «Habilitation à Diriger des Recherches» degree from the University of Paris-Sud in March 2014. He is a Professor with CentraleSupelec, Gif Sur Yvette, France. He is currently with GeePs (Group of Electrical Engineering, Paris), Paris, France. His current research interests include electromagnetic modeling, electromagnetic compatibility, and power electronics, including modeling, simulation, and instrumentation.